14th European Signal Processing Conference (EUSIPCO 2006), Florence, Italy, September 4-8, 2006, copyright by EURASIP

LOSSLESS COMPRESSION OF BAYER MASK IMAGES USING AN OPTIMAL VECTOR PREDICTION TECHNIQUE

Stefano Andriani, Giancarlo Calvagno and Daniele Menon

Dept. of Information Engineering, University of Padova
via Gradenigo 6/b, 35100, Padova, Italy
phone: + 39 049 827 7641, fax: + 39 049 827 7699,
email: {stefano.andriani,calvagno,daniele.menon}@dei.unipd.it
web: www.dei.unipd.it

ABSTRACT

In this paper a lossless compression technique for Bayer pattern images is presented. The common way to save these images was to colour reconstruct them and then code the full resolution images using one of the lossless or lossy methods. This solution is useful to show the captured images at once, but it is not convenient for efficient source coding. In fact, the resulting full colour image is three times greater than the Bayer pattern image and the compression algorithms are not able to remove the correlations introduced by the reconstruction algorithm. However, the Bayer pattern images present new problems for the coding step. In fact, adjacent pixels belong to different colour bands mixing up different kinds of correlations. In this paper we present a lossless compression procedure based on an optimal vector predictor, where the Bayer pattern is divided into non-overlapped 2×2 *blocks, each of them predicted as a vector. We show that this solution is able to exploit the existing correlation giving a good improvement of the compression ratio with respect to other lossless compression techniques, e.g., JPEG-LS.*

1. INTRODUCTION

Most digital cameras produce colour images using a single CCD sensor provided by a colour filter array (CFA). In this way, adjacent pixels capture the light intensity value of different colour bands, and a full colour image is obtained by a colour interpolation step which reconstructs the missing values.

The Bayer pattern, presented by Bayer in [1], is the most popular and used colour filter array (CFA). It uses a rectangular grid for the red and blue bands and a quincunx grid for the green band, as shown in Fig. 1. The choice of capturing a number of green pixels twice as high as the red and the blue bands is justified by the fact that the Human Visual System (HVS) places more emphasis on the green rather then on the red and blue components.

The common way to manage the Bayer pattern images is to colour reconstruct them, applying automatic white balancing and other colour corrections, and then compress the resulting images. This workflow is effective for most digital camera users, but the professional photographers demand for custom post-processing of the captured images. To achieve this requirement, the professional digital photo cameras allow for saving the raw sensor data without any post-processing step. This option permits the advanced user to apply high-complexity high-quality demosaicing algorithms during a post-processing step. Until now, each captured image has been saved in a RAW format without any compression step, and only Nikon proposes a visually, but not numerically, lossless coder called NEF (Nikon Electronic Format). This solution satisfies the user requirement, but limits the number of pictures which could be saved into the flash memory card of the camera. Besides, if we consider the cost of this kind of memory, the need of a good lossless compression technique is gaining importance day by day.

Figure 1: Bayer pattern used in the paper.

In literature, the first works on this issue were developed by S. Lee and A. Ortega in [2] and C.C. Koh and S.K. Mitra in [3]. The first paper proposes that the compression step is placed before the colour reconstruction algorithm. The authors propose an image transformation algorithm to reduce the existing redundancy in a CFA image and then they code the transformed image using JPEG.

Mitra *et al* propose new image transformations to be applied to the Bayer image before the JPEG compression step. They code the red and blue bands without any transformation because these bands have a rectangular array suitable for JPEG. The transformations are applied only on the green band where a quincunx sampling is used. They propose two methods: the first uses a diamond filter with a 2-D impulse response and then the data is separated into odd and even components independently coded. In the second method the columns of the quincunx array are collapsed into a compact array. This operation creates false high frequencies in both the horizontal and vertical directions. To reduce this effect the quincunx data has been thought as two interlaced frames of a scene, so through the process of deinterlacing a smooth image is obtained.

Unfortunately, these approaches introduce some loss. A lossless compression algorithm for the color mosaic images is proposed by N. Zhang and X. Wu in [4]. They use the lifting integer wavelet to decorrelate the mosaic data both in spatial and spectral domains. Then the integer transform

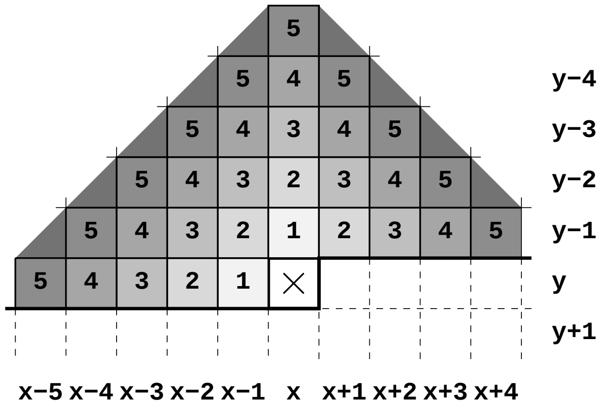

Figure 2: Manhattan distance (MD) of the neighbour pixels to the current one.

coefficients are coded by a simple context-based Golomb-Rice coding scheme.

Our approach uses a DPCM mechanism to decorrelate the mosaic colour images, where the optimal prediction is estimated using the causal adjacent pixels given by a raster scan order. However, the Bayer pattern images are not considered as grayscale images, but as non-overlapped block images where each block contains two green, one red and one blue samples. For each prediction step we estimate an image block (i.e., four image adjacent samples) using the optimal *vector* prediction theory. In this way, our predictor is able to exploit both the spatial and spectral correlation and uses them to improve the prediction performance (reducing the prediction error entropy).

The paper is organized as follows. Section 2 presents the proposed coding scheme, and its experimental results are shown in Section 3. In Section 4 we report the conclusion of this work.

2. PROPOSED ALGORITHMS

In one-dimension the m-order one-step linear predictor of a signal x at time n is given by

$$\hat{x}(n) = \sum_{i=1}^{m} w_i x(n-i)$$

where $x(n-i)$ are past observations of the signal, and w_i are the prediction coefficients.

The predictor is called *optimal* if the prediction coefficients w_i minimize the energy of the prediction error:

$$e(n) = x(n) - \hat{x}(n) = x(n) - \sum_{i=1}^{m} w_i x(n-i).$$

From the orthogonality principle, this condition is verified if and only if the prediction error is orthogonal to the past signal observations.

2.1 Optimal Scalar Prediction (OSP)

For image prediction we must address a two-dimensional problem. The first issue is to define the set of the neighbour (causal) pixels which define the previous samples of the optimal predictor.

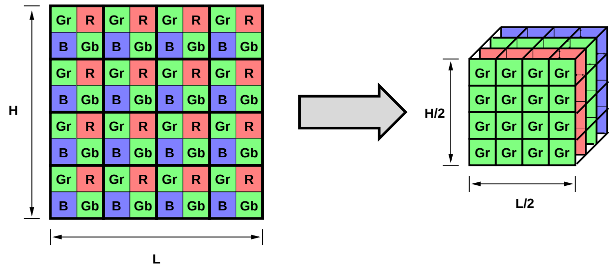

Figure 3: Prediction blocks.

Using a raster scan order, one solution to this problem could be given by the set of pixels having Manhattan distance smaller than a fixed threshold T_s (see Fig. 2). Let $p(x,y)$ be the pixel value at position (x,y), then the prediction set $\mathscr{P}_{x,y}^{T_s}$ of this pixel is given by:

$$\mathscr{P}_{x,y}^{T_s} = \left\{ p(x-k, y-j) : (k,j) \in \mathscr{A}_{k,j} \wedge |k| + |j| \leq T_s \right\}$$

where

$$\mathscr{A}_{k,j} = \{k \in \mathbb{Z},\ j \in \mathbb{N}_0 : (k \in \mathbb{Z}, j > 0) \vee (k > 0, j = 0)\}.$$

$\mathscr{A}_{k,j}$, $\mathbb{N}_0$ and $\mathbb{Z}$ are the sets of the previous causal pixel, of the natural and of the integer numbers, respectively.

The threshold value T_s fixes the predictor order, so if it is high the prediction set $\mathscr{P}_{x,y}^{T_s}$ has an high cardinality, and we have an high-order predictor. This solution works well if we predict a natural image where there are smooth changes of luminance value, but for synthetic images this solution does not work well because the luminance could change in strange (and unpredictable) ways. On the other hand, if the threshold is too low, we obtain a low order predictor which works well on the edges, but not so well on smooth region.

To predict the pixel $p(x,y)$ we use the previous coded pixels according to the scan order introduced in Fig. 2.

The optimal prediction coefficients $w_{x,y,k}$ are adaptively computed solving the linear system

$$\mathbf{R}_{x,y}\mathbf{w}_{x,y} = \mathbf{R}_{0,x,y}, \tag{1}$$

where $\mathbf{R}_{x,y}$ is an estimate of the autocorrelation matrix, and $\mathbf{R}_{0,x,y}$ is a correlation vector. At the end, the predicted pixel $\hat{p}(x,y)$ is computed according to

$$\hat{p}(x,y) = \sum_{k=1}^{m} w_{x,y,k}\ p_{x,y,k} \tag{2}$$

where $p_{x,y,k} \in \mathscr{P}_{x,y}^{T_s}$.

To compute the optimal predictor, the autocorrelation matrix is needed. We estimate it using the covariance method taking into account only the actual coded pixels. In this way, the estimate of the autocorrelation matrix for the pixel at position (x,y) is given by

$$\mathbf{R}_{x,y} = \sum_{j=0}^{y-1}\sum_{k=0}^{L-1} \alpha^{|x-k|-|y-j|}\mathbf{A}_{k,j} + \sum_{k=0}^{x-1} \alpha^{|x-k|}\mathbf{A}_{k,y}, \tag{3}$$

and the vector $\mathbf{R}_{0,x,y}$ by

$$\mathbf{R}_{0,x,y} = \sum_{j=0}^{y-1}\sum_{k=0}^{L-1} \alpha^{|x-k|-|y-j|}\mathbf{A}_{0,k,j} + \sum_{k=0}^{x-1} \alpha^{|x-k|}\mathbf{A}_{0,k,y}, \tag{4}$$

where L is the width of the image, and α is an empirical weight introduced to decrease the influence of the farthest pixels from the current position (x,y).

To build up the matrix $\mathbf{A}_{x,y}$ and the vector $\mathbf{A}_{0,x,y}$ we define the vector $\mathbf{p}_{x,y}$ as

$$\mathbf{p}_{x,y} = \begin{bmatrix} p_{x,y,1} \\ p_{x,y,2} \\ \vdots \\ p_{x,y,m} \end{bmatrix}, \tag{5}$$

where the components $p_{x,y,1}, \dots, p_{x,y,m}$ belong to the prediction set $\mathscr{P}_{x,y}^{T_s}$, and m is the order of the predictor, i.e., the cardinality of $\mathscr{P}_{x,y}^{T_s}$.

From $\mathbf{p}_{x,y}$, the matrix $\mathbf{A}_{x,y}$ and the vector $\mathbf{A}_{0,x,y}$ are computed according to

$$\begin{aligned}\mathbf{A}_{x,y} &= \mathbf{p}_{x,y}\mathbf{p}_{x,y}^t \\ &= \begin{bmatrix} p_{x,y,1}^2 & p_{x,y,1}p_{x,y,2} & \cdots & p_{x,y,1}p_{x,y,m} \\ p_{x,y,1}p_{x,y,2} & p_{x,y,2}^2 & \cdots & p_{x,y,2}p_{x,y,m} \\ \vdots & \vdots & \ddots & \vdots \\ p_{x,y,1}p_{x,y,m} & p_{x,y,2}p_{x,y,m} & \cdots & p_{x,y,m}^2 \end{bmatrix},\end{aligned}$$

$$\mathbf{A}_{0,x,y} = p(x,y)\mathbf{p}_{x,y} = \begin{bmatrix} p(x,y)p_{x,y,1} \\ p(x,y)p_{x,y,2} \\ \vdots \\ p(x,y)p_{x,y,m} \end{bmatrix},$$

where $\mathbf{A}_{x,y}$ is a symmetric positive definite matrix, but not a Toeplitz matrix.

2.2 Optimal Vector Prediction (OVP)

To extend the linear prediction to the vector case we divide the Bayer pattern image into non-overlapping 2×2 blocks considering the pixels belonging to each block as the components of a single pixel vector. The resulting block image has a dimension equal to $L/2 \times H/2$ where L and H are the width and the height of the original image, respectively (see Fig 3).

Each block is composed by two green, one red and one blue pixels. To distinguish the two green pixels we denote with G_r and G_b the green samples which belong, respectively, to the odd and to the even rows of the Bayer pattern reported in Fig. 1.

Let $\bar{\mathbf{p_b}}(x,y)$ be the vector of the block at position (x,y)

$$\bar{\mathbf{p_b}}(x,y) = \left[R_{x,y} \quad G_{r,x,y} \quad G_{b,x,y} \quad B_{x,y}\right], \tag{6}$$

where the coordinate (x,y) refers to the block and not to the pixel position.

To predict this vector we use the causal blocks having Manhattan distance smaller or equal than a fixed threshold T_v. Accordingly, the prediction set is given by

$$\bar{\mathscr{P}}_{x,y}^{T_v} = \left\{\bar{\mathbf{p_b}}(x-k, y-j) : (k,j) \in \mathscr{A}_{k,j} \wedge |k| + |j| \le T\right\}$$

where $\mathscr{A}_{k,j}$ is the set of the causal blocks in raster scan order.

In this paper, we consider a single threshold $T_v = 2$ having $\bar{\mathscr{P}}_{x,y}^2$ as prediction sets with a block cardinality equal to six.

To predict the pixel vector $\bar{\mathbf{p}}(x,y)$ we use the previous coded pixel vectors according to the scan order introduced in Fig. 2.

To estimate the autocorrelation matrix we write the vector of the causal block as

$$\mathbf{p}_{x,y} = \left[\bar{\mathbf{p_b}}_{x,y,1} \quad \bar{\mathbf{p_b}}_{x,y,2} \quad \cdots \quad \bar{\mathbf{p_b}}_{x,y,m}\right]^t, \tag{7}$$

where m is the cardinality of the prediction set. From $\mathbf{p}_{x,y}$ the two matrices $\mathbf{A}_{x,y}$ and $\mathbf{A}_{0,x,y}$ are computed according to

$$\begin{aligned}\mathbf{A}_{x,y} &= \mathbf{p}_{x,y}\mathbf{p}_{x,y}^t \qquad (8) \\ &= \begin{bmatrix} \bar{\mathbf{A}}_{x,y,1,1} & \bar{\mathbf{A}}_{x,y,1,2} & \cdots & \bar{\mathbf{A}}_{x,y,1,m} \\ \bar{\mathbf{A}}_{x,y,2,1} & \bar{\mathbf{A}}_{x,y,2,2} & \cdots & \bar{\mathbf{A}}_{x,y,2,m} \\ \vdots & \vdots & \ddots & \vdots \\ \bar{\mathbf{A}}_{x,y,m,1} & \bar{\mathbf{A}}_{x,y,m,2} & \cdots & \bar{\mathbf{A}}_{x,y,m,m} \end{bmatrix},\end{aligned}$$

$$\begin{aligned}\mathbf{A}_{0,x,y} &= [\bar{\mathbf{p_b}}(x,y)\mathbf{p}_{x,y}]^t \qquad (9) \\ &= [\ R_{x,y}\mathbf{p}_{x,y} \mid G_{r,x,y}\mathbf{p}_{x,y} \mid G_{b,x,y}\mathbf{p}_{x,y} \mid B_{x,y}\mathbf{p}_{x,y}\ ],\end{aligned}$$

where $\mathbf{A}_{x,y}$ is a block symmetric matrix, but not block Toeplitz. Each block $\bar{\mathbf{A}}_{x,y,i,j}$ represents the existing spatial and spectral correlation between the two pixel vectors $\bar{\mathbf{p_b}}(x,y,i)$ and $\bar{\mathbf{p_b}}(x,y,j)$ which belong to the prediction set.

The estimate of the autocorrelation matrix $\mathbf{R}_{x,y}$ and of matrix $\mathbf{R}_{0,x,y}$ is made as in (3) and (4), respectively. In optimal vector theory, the prediction block coefficients $\mathbf{w}_{x,y,k}$ are 4×4 matrices which are adaptively computed solving the linear systems

$$\mathbf{R}_{x,y}\mathbf{W}_{x,y} = \mathbf{R}_{0,x,y}, \tag{10}$$

where

$$\mathbf{W}_{x,y} = \begin{bmatrix} \mathbf{w}_{x,y,1} \\ \mathbf{w}_{x,y,2} \\ \vdots \\ \mathbf{w}_{x,y,m} \end{bmatrix},$$

and the predicted pixel vector $\hat{\bar{\mathbf{p_b}}}(x,y)$ is computed according to

$$\hat{\bar{\mathbf{p}}}(x,y) = \sum_{k=1}^{m} \mathbf{w}_{x,y,k}\, \bar{\mathbf{p_b}}_{x,y,k}. \tag{11}$$

To summarize, for each prediction the following steps have to be performed:

1. update the vector $\mathbf{p}_{x,y}$ (7), and the two matrices $\mathbf{A}_{x,y}$ (**??**) and $\mathbf{A}_{0,x,y}$ (9);
2. estimate the autocorrelation matrix $\mathbf{R}_{x,y}$ (3), and the correlation matrix $\mathbf{R}_{0,x,y}$ (4);
3. invert the autocorrelation matrix $\mathbf{R}_{x,y}$ to obtain the prediction coefficient vector
$$\mathbf{W}_{x,y} = (\mathbf{R}_{x,y})^{-1}\,\mathbf{R}_{0,x,y}; \tag{12}$$
4. calculate the predicted pixel vector $\hat{\bar{\mathbf{p_b}}}(x,y)$ by (11).

To reduce the complexity of the second step we use the matrix update method introduced by [5], where the high computational cost problem is turned to a high memory requirement problem. To calculate the inverse matrix of $\mathbf{R}_{x,y}$ we use the Cholesky factorization obtaining a computational cost order equal to $\mathscr{O}((4m)^3/6)$.

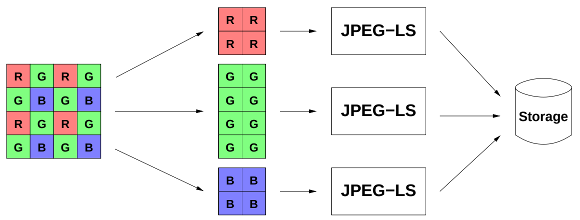

Figure 4: JPEG-LS applied on the three colour components obtained by a Bayer pattern splitting.

The pixel vector value $\bar{\mathbf{p}}_{x,y}$ is then coded through an arithmetic binary coder in bit-plane mode starting from the MSB down to the LSB, and the zero's probability is computed modelling the prediction error

$$\mathbf{e}_{x,y} = \bar{\mathbf{p}}_{x,y} - \hat{\bar{\mathbf{p}}}_{x,y}$$

by a modified Student's distribution centered on the predicted pixel value [5].

Since each frame is extended to a constant value outside the image boundaries, the decoder can replicate the coder operations without requiring that the predictor coefficients are sent as side-information.

3. RESULTS

We tested our algorithm using the reference Kodak set images, and the three test images called *Woman*, *Bike* and *Monarch*. These images have a 24-bit colour representation, and were sampled according to the Bayer pattern shown in Fig. 1.

We compare our algorithm with respect to the standard lossless coder JPEG-LS presented in [6] and implemented by HP Laboratories[1]. We tested JPEG-LS on Bayer pattern images in two ways:

1. directly applying JPEG-LS to the Bayer pattern images;
2. applying JPEG-LS to the three colour components obtained splitting the Bayer pattern images, as show in Fig. 4.

From the results reported in Table 1 we can conclude that applying the JPEG-LS coder directly to the Bayer pattern images is not a good solution. In fact, JPEG-LS is provided with a very simple but effective predictor called MED (Median Edge Detector). This predictor checks for the presence of vertical or horizontal edges predicting along them when they occur, otherwise it estimates the current pixel as the mean value of the adjacent pixels. In the Bayer pattern images (BPI) adjacent pixels always present abrupt intensity changes due to the fact that they belong to different colour components. For this reason, the MED predictor is not able to detect edges, becoming a very simple and ineffective mobile average filter.

To obtain the results reported in the second column of Table 1 we split the Bayer pattern images into three different images representing the three colour components (see Fig. 4). In this way, we obtain a compression gain, with respect to the first solution, roughly equal to 0.7 bit per pixel. The same gain (refer to the third column of Table 1) is obtained applying the lossless mode of JPEG2000 directly to the Bayer pattern images. As said in [4], this result is due to the reversible 5-3 integer discrete wavelet transform which de-correlates the mosaic data both in the spatial and spectral domains.

For the optimal scalar predictor we used two different thresholds $T_s = \{2,3\}$ and the corresponding prediction sets $\mathscr{P}_{x,y}^{\{2,3\}}$ have cardinality equal to 6 and 12, respectively. On the other hand, for the optimal vector predictor we fixed the threshold equal to 2 ($T_v = 2$) obtaining a prediction set $\underline{\mathscr{P}}_{x,y}^{2}$ having a block cardinality equal to 6 where each block consists of four pixels. The thresholds for the OSP algorithm are selected considering that with $T_s = 2$ the scalar and the vectorial predictor have the same threshold value, and with $T_s = 3$ the two coders have the same complexity.

The OVP coder works better than the OSP coders ($T_s = 2$ and $T_s = 3$) because it organizes the pixels into a well-defined structure where both the spatial and the spectral correlations are exploited. On the other hand, in the OSP coders, the raster scan over a Bayer pattern image implies a repetitive exchange between the position of the spectral and the spatial correlation inside the prediction vector $\mathbf{p}_{x,y}$ and then inside the estimate of the autocorrelation matrix used to calculate the prediction weights. For this reason, the structure of the OVP coder leads to higher compression ratios. However, it is worth to note that the OSP coders applied to the Bayer pattern images achieve better results with respect to appling independently the same algorithms to the Bayer splitted images. This results lead us to conclude that also the OSP coders exploits both spectral and spatial correlations, but not as efficiently as the OVP coder.

Finally, we compare the proposed optimal vector prediction algorithm with respect to other lossless coders presented in literature, namely: JPEG-LS independently applied on the three colour components obtained splitting the Bayer data, JPEG2000 applied on the Bayer pattern image, and the coder presented by Zhang and Wu in [4].

The performance improvement of the proposed algorithm is about 0.4 bpp with respect to the standard lossless coder JPEG-LS, and 0.2 bpp with respect to the Zhang and Wu algorithm. However, the complexity of the proposed algorithm is too high to allow for a real-time implementation. This high computational cost is due to two main reasons: the first is that we have to invert a 24×24 autocorrelation matrix $\mathbf{R}_{x,y}$ for each block prediction; the second is due to the estimate of the zero probability by numerical integration of the modified Student distribution.

4. CONCLUSION

In this paper we propose a new lossless compression algorithm based upon the optimal vector prediction theory. The Bayer pattern is divided into 2×2 non-overlapping blocks containing two green, one red and one blue pixels. Each block is then predicted exploiting the spatial and the spectral correlations existing between pixels which belong to the same block and to the adjacent causal blocks. The obtained results show that the proposed method is effective, but its complexity is too high to allow for a real-time on-board hardware implementation, so the captured images have to be saved in RAW format on the flash memory of the camera and then compressed in a post-processing step.

[1] http://www.hpl.hp.com/research/info_theory/loco/

Image	JPEG-LS		JPEG2000	Zhang and Wu	Optimal Spatial Predictor				Optimal
	Bayer Pattern	RGB			$T_s = 2$		$T_s = 3$		Vector
	Image (BPI)	Splitted	[7]	[4]	BPI	RGB	BPI	RGB	Predictor
Woman	5.59	5.16	4.94	4.88	4.76	4.96	4.71	4.92	4.65
Bike	5.79	4.99	5.05	4.91	4.72	4.98	4.64	4.89	4.60
Monarch	7.21	4.45	4.89	4.38	4.39	4.39	4.25	4.34	4.11
KD01	6.39	5.97	5.81	5.65	5.70	5.90	5.55	5.87	5.51
KD06	5.86	5.15	5.21	5.03	4.98	5.12	4.83	5.10	4.67
KD08	6.29	6.19	5.90	5.73	5.63	6.05	5.49	5.99	5.60
KD13	6.73	6.48	6.37	6.24	6.23	6.35	6.17	6.35	6.07
KD19	5.69	5.12	4.91	4.82	4.77	4.90	4.69	4.87	4.61
KD21	5.47	5.00	5.03	4.87	4.85	4.94	4.79	4.92	4.71
Average	6.11	5.39	5.35	5.17	5.11	5.28	5.01	5.25	4.96

Table 1: Comparison between different Bayer pattern lossless coders.

REFERENCES

[1] Bryce E. Bayer, "Color Imaging Array," U.S. patent, 3,971,065, 1976.

[2] S. Lee and A. Ortega, "A novel approach of image compression in digital cameras with a Bayer color filter array," in *Proc. IEEE International Conference on Image Processing (ICIP 2001)*, Thessaloniki, Greece, Oct. 2001, pp. 482–485.

[3] C.C. Koh and S.K. Mitra, "Compression of Bayer color filter array data," in *Proc. IEEE International Conference on Image Processing (ICIP 2003)*, Barcellona, Spain, Sep. 2003.

[4] N. Zhang and X. Wu, "Lossless compression of color mosaic images," in *Proc. IEEE International Conference on Image Processing (ICIP 2004)*, Singapore, Oct. 2004, pp. 517–520.

[5] B. Meyer and P.E. Tischer, "GLICBAWLS - Grey Level Image Compression By Adaptive Weighted Least Squares," in *Proc. Data Compression Conference (DCC 2001)*, Snowbird, Utah, USA, Mar. 2001, p.503.

[6] M.J. Weinberger and G. Seroussi and G. Sapiro, "The LOCO-I Lossless Image Compression Algorithm: Principles and Standardization into JPEG-LS," *IEEE Trans. Image Processing*, vol. 9, no. 8, pp. 1309–1324, Aug. 2000.

[7] D.S. Taubman and M.W. Marcellin, *JPEG2000 Image compression, fundamentals, standards and practice*, Kluwer Academic Publishers, 2002.